A fast SOI-based variable optical attenuator with a p-i-n structure with low polarization dependent loss*

YUAN Pei (袁配)[1], **WU Yuan-da** (吴远大)[2], **WANG Yue** (王玥)[2]**, **AN Jun-ming** (安俊明)[2], and **HU Xiong-wei** (胡雄伟)[2]

1. Henan Shi Jia Photons Technology Co., Ltd., Hebi 458030, China

2. State Key Laboratory on Integrated Optoelectronics, Institute of Semiconductors, Chinese Academy of Sciences, Beijing 100083, China

(Received 23 November 2015)

According to the plasma dispersion effect of silicon (Si), a silicon-on-insulator (SOI) based variable optical attenuator (VOA) with p-i-n lateral diode structure is demonstrated in this paper. A wire rib waveguide with sub-micrometer cross section is adopted. The device is only about 2 mm long. The power consumption of the VOA is 76.3 mW (0.67 V, 113.9 mA), and due to the carrier absorption, the polarization dependent loss (*PDL*) is 0.1 dB at 20 dB attenuation. The raise time of the VOA is 34.5 ns, the fall time is 37 ns, and the response time is 71.5 ns.

Document code: A **Article ID:** 1673-1905(2016)01-0020-3

DOI 10.1007/s11801-016-5234-z

Dense wavelength division multiplexing (DWDM) technology through optical fibers is the main solution to the current explosive growth of communication. Monolithic photonics integration[1-4] is obviously the trend to achieve cost-effective optical devices. For example, the monolithic integration of arrayed waveguide grating (AWG)[5-7] acting as the wavelength division multiplexing/demultiplexing device and variable optical attenuator (VOA)[8-10] acting as the optical power equalization device are the key devices to realize low-cost wavelength division multiplexing (WDM) systems. The fabrication process of planar lightwave circuit (PLC) type VOA is compatible with the mature silicon (Si) integrated circuit (IC) manufacturing process, and makes it possible to integrate two kinds of devices (such as lasers[11-13] and modulators[14,15]) on a single chip.

Many types of VOAs have been reported before. The thermo-optic VOA[9,10] based on Mach-Zehnder interferometer (MZI) always has low respond rate, high power consumption and high polarization dependent loss (*PDL*) caused by the waveguide birefringence.

Electrical absorption (EA) type VOAs[16,17] with large cross-section (generally a few micrometers) and p-i-n structure have an advantage over the thermo-optic VOAs, but this kind of VOAs have a large size, and their power consumption can be up to several hundred microwatts.

In this paper, a silicon-on-insulator (SOI) VOA based on wire rib waveguide with sub-micrometer cross section is reported. The device is only about 2 mm long, and it is easy to form a compact VOA array.

The plasma dispersion effect of Si at wavelength of 1.55 μm can be depicted by

$$\Delta n=-[8.8\times10^{-22}\Delta N_e+8.5\times10^{-18}(\Delta N_h)^{0.8}], \quad (1)$$

$$\Delta\alpha=8.5\times10^{-18}\Delta N_e+8.5\times10^{-18}\Delta N_h, \quad (2)$$

where ΔN_e and ΔN_h represent the concentration of electrons and holes, respectively, and Δn and $\Delta\alpha$ is the increment in the refractive index and absorption coefficient, respectively.

Fig.1 shows the structure diagram of VOA based on SOI. As can be seen from Fig.1(a) and (b), phosphorus and boron are doped in either side of the waveguide core to form a lateral p-i-n structure. When the forward bias is applied on the Al pad, the carriers will be injected into the i-zone, resulting in the increase of absorption coefficient ($\Delta\alpha$) according to Eq.(2) and the attenuation of power of light wave.

In this design, the refractive indices of Si and SiO_2 are 3.478 and 1.445, respectively. The thicknesses of the buried oxide layer and the cap layer are both 1 μm, the thickness of top Si is 220 nm, the width of the waveguide is 500 nm, and the thickness of the slab is 70 nm to ensure the single-mode propagation. The length of P+ and N+ zone is 1 mm, and the distance between P+ and N+ zone is 3 μm. A spot-size converter (SSC) is used as shown in Fig.1(b) to decrease the coupling loss caused by the mode-size mismatch between the input/output fiber and the VOA input/output waveguides.

* This work has been supported by the National High Technology Research and Development Program of China (No.2013AA031402).

** E-mail: wy1022@semi.ac.cn

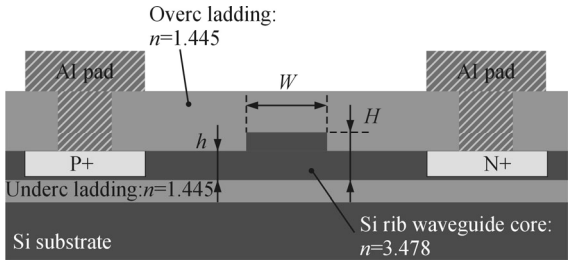

(a) Cross-sectional view of the VOA

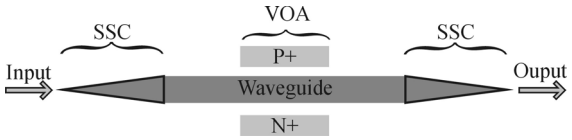

(b) Top view of the VOA

Fig.1 The structure diagram of VOA based on SOI

For the fabrication of VOA, at first, deep ultra-violet lithography (DUVL) was used to form the mask layer for the Si etching. Then, the Si core was fabricated by the inductively coupled plasma (ICP) etching to a depth of 70 nm. Then the ion implantations of boron and phosphorus with the density of 5.5×10^{20} cm^{-3} were done respectively to form P+ and N+ regions. Next, the cladding layer was fabricated by plasma-enhanced chemical vapor deposition (PECVD), and the contacting hole was fabricated by photolithography and ICP etching. After that, aluminum (Al) was deposited by the sputter and lift-off technology to form the electrodes. At last, the annealing technology was used to activate the carriers.

Fig.2 shows some partial micrographs and scanning electron microscope (SEM) image of the VOA.

A coupling test platform was used to do the measurements. The light from a broadband amplified spontaneous emission (ASE) source was linearized by a polarizer and adjusted to the transverse electric (TE) mode or the transverse magmatic (TM) mode by a polarization controller. Then the TE or TM mode was input to the VOA, and the output light from the VOA was measured by an optical power meter and a spectrum analyzer. The direct current (DC) source was contacted to the Al pad to do the electrical measurements.

The dependence of attenuation on the injected current is shown in Fig.3, which exhibits a linear relationship between the attenuation and the injected current, and the

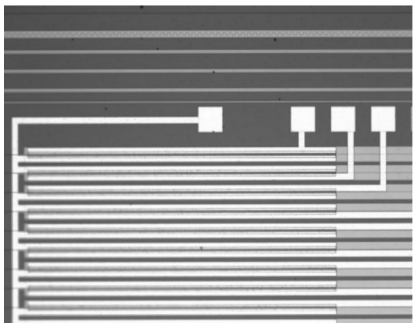

(a) The micrograph of the VOA electrodes with magnification of 1 000×

(b) The micrograph of the SSC with magnification of 1 000×

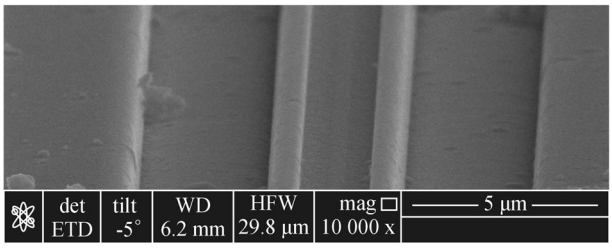

(c) The SEM image of the waveguide

Fig.2 Some partial micrographs and SEM image of the VOA

attenuation can be 0—20 dB. From Fig.3 we can see that the VOA becomes more attenuated as the injected current increases. The injected currents are 57.2 mA and 113.9 mA at attenuation of 10 dB and 20 dB, respectively, and the power consumption is 76.3 mW (0.67 V, 113.9 mA) at attenuation of 20 dB.

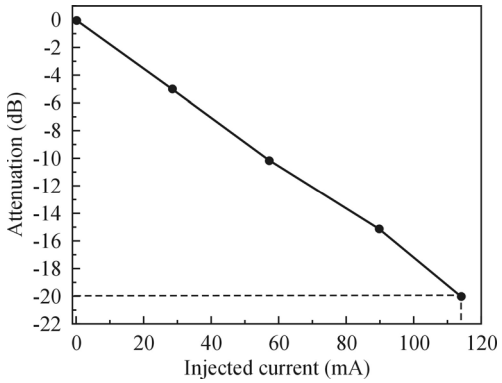

Fig.3 The dependence of attenuation on the injected current

As we all know, when there is an absorption occurring, the TE mode and the TM mode have a complex effective index (N_{eff}), which is expressed as

$$N_{\text{eff}}=n+\text{i}k, \tag{3}$$

where n and k are the real part and the imaginary part of the effective refractive index, respectively. The relationships between absorption coefficient and the effective refractive index imaginary part of the two modes (k_{TE} and k_{TM}) are written as

$$TE_{\text{att}}=10\log\left[\exp\left(\frac{-4\pi k_{\text{TE}}L}{\lambda}\right)\right], \tag{4}$$

$$TM_{\text{att}}=10\log\left[\exp\left(\frac{-4\pi k_{\text{TM}}L}{\lambda}\right)\right], \tag{5}$$

where TE_{att} and TM_{att} represent the attenuation of TE and TM polarization by carrier absorption, λ is the operation wavelength, and L is the length of VOA. The *PDL* due to

free-carrier absorption is given as[18]

$$PDL=|TE_{att}-TM_{att}|. \quad (6)$$

Fig.4 shows the dependences of the attenuation for the two polarizations (TE mode and TM mode) and $|TE_{att}-TM_{att}|$ (PDL) on the injected current. We can see from Fig.4 that the PDL due to the carrier absorption is 0.1 dB at 20 dB attenuation.

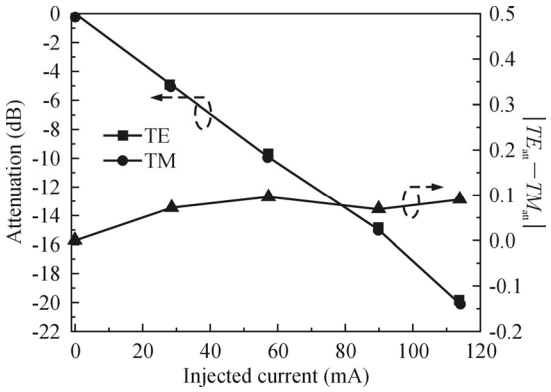

Fig.4 The dependences of the attenuation for the two polarizations (TE mode and TM mode) and $|TE_{att}-TM_{att}|$ on the injected current

For measuring the response time, the anode and the cathode of the waveform generator are connected to those of the VOA device and the oscilloscope, so that the square signal generated by a waveform generator is input to the oscilloscope and the VOA. At the same time, the output light from the VOA is inputted to a photoelectric detector through an output fiber, and the detector is connected with the oscilloscope.

Fig.5 shows the measured response time of the VOA when a 1 MHz square signal is applied. We can see that the raise time of the VOA is 34.5 ns, the fall time is 37 ns, and the response time is 71.5 ns.

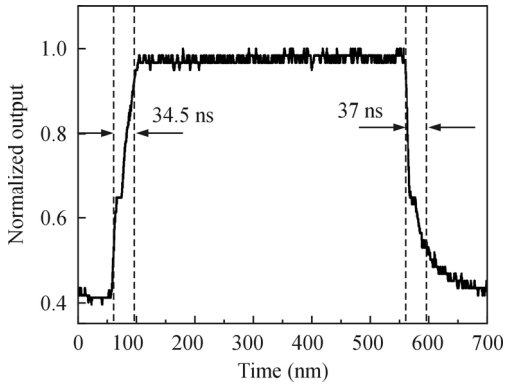

Fig.5 The measured response time of the VOA

In this paper, we develop an SOI VOA based on a p-i-n structure with a sub micrometer cross section. The VOA has low *PDL* of 0.1 dB due to free-carrier absorption. The power consumption of the VOA at 20 dB attenuation is 76.3 mW (0.67 V, 113.9 mA). The raise time of the VOA is 34.5 ns, the fall time is 37 ns, and the response time is 71.5 ns. The device is only about 2 mm long, and it is easy to form a compact VOA array.

References

[1] Hidetaka Nishi, Tai Tsuchizawa, Toshifumi Watanabe, Hiroyuki Shinojima, Sungbong Park, Rai Kou, Koji Yamada and Sei-ichi Itabashi, Applied Physics Express **3**, 102203 (2010).

[2] Dai Hongqing, An Junming, Wang Yue, Zhang Jiashun, Wang Liangliang, Wang Hongjie, Li Jianguang, Wu Yuanda, Zhong Fei and Zha Qiang, Journal of Semiconductors **35**, 104010-1 (2014).

[3] Dazeng Feng, Ning-Ning Feng, Cheng-Chih Kung, Hong Liang, Wei Qian, Joan Fong, B. Jonathan Luff and Mehdi Asghari, Optics Express **19**, 6125 (2011).

[4] Yuan Pei, Wu Yuanda, Wang Yue, An Junming and Hu Xiongwei, Journal of Semiconductors **36**, 084005 (2015).

[5] Nurjuliana Juhari, P Susthitha Menon, Abang Annuar Ehsan and Sahbudin Shaari, Journal of Nonlinear Optical Physics & Materials **23**, 1450008 (2014).

[6] Tong Ye, Yunfei Fu, Lei Qiao and Tao Chu, Optics Express **22**, 31899 (2014).

[7] Zhang Jiashun, An Junming, Zhao Lei, Song Shijiao, Wang Liangliang, Li Jianguang, Wang Hongjie, Wu Yuanda and Hu Xiongwei, Journal of Semiconductors **32**, 044009 (2011).

[8] You Min Chang, Junsu Lee, Young Min Jhon and Ju Han Lee, Optics Express **19**, 26911 (2011).

[9] Pengfei Qu, Weiyou Chen, Fumin Li, Caixia Liu and Wei Dong, Optics Express **16**, 20334 (2008).

[10] Kei Watanabe, Yasuaki Hashizume, Yusuke Nasu, Masaki Kohtoku, Mikitaka Itoh and Yasuyuki Inoue, Journal of Lightwave Technology **26**, 2235 (2008).

[11] Cong Chen, Zhi-wei Xu, Meng Wang and Hai-yan Chen, Optoelectronics Letters **10**, 427 (2014).

[12] Juan Zhang, Ling-zhen Yang, Nai-jun Xu, Juan-fen Wang, Zhao-xia Zhang and Xiang-lian Liu, Optoelectronics Letters **10**, 232 (2014).

[13] Shinsuke Tanaka, Seok-Hwan Jeong, Shigeaki, Sekiguchi, Teruo Kurahashi, Yu Tanaka and Ken Morito, Optics Express **20**, 28057 (2012).

[14] Jianfeng Ding, Hongtao Chen, Lin Yang, Lei Zhang, Ruiqiang Ji, Yonghui Tian, Weiwei Zhu, Yangyang Lu, Ping Zhou, Rui Min and Mingbin Yu, Optics Express **20**, 70811 (2012).

[15] Yang Liu and Guo-an Zhang, Optoelectronics Letters **10**, 273 (2014).

[16] He Yue-Jiao, Li Fang and Liu Yu-Liang, Chinese Physics Letter **22**, 95 (2005).

[17] Qingfeng Yan, Jinzhong Yu, Jinsong Xia and Zhongli Liu, Chinese Optics Letters **1**, 217 (2003).

[18] Hidetaka Nishi, Tai Tsuchizawa, Toshifumi Watanabe, Hiroyuki Shinojima, Koji Yamada and Sei-ichi Itabashi, Japanese Journal of Applied Physics **49**, 04DG20 (2010).